Original Article

Serial assessment of iron in the motor cortex in limb-onset amyotrophic lateral sclerosis using quantitative susceptibility mapping

Anjan Bhattarai[1,2], Zhaolin Chen[2], Phillip G. D. Ward[2], Paul Talman[3], Susan Mathers[4,5], Thanh G. Phan[5], Caron Chapman[4], James Howe[4], Sarah Lee[4], Yennie Lie[4], Gary F. Egan[2], Phyllis Chua[1,4]

[1]Department of Psychiatry, School of Clinical Sciences at Monash Health, Monash University, Clayton, Victoria, Australia; [2]Monash Biomedical Imaging, Monash University, Clayton, Victoria, Australia; [3]Department of Neuroscience, Barwon Health, Geelong, Victoria, Australia; [4]Statewide Progressive Neurological Services, Calvary Health Care Bethlehem, South Caulfield, Victoria, Australia; [5]Department of Neurology, Monash Health, and School of Clinical Sciences at Monash Health, Monash University, Clayton, Victoria, Australia

Correspondence to: Anjan Bhattarai. Monash Biomedical Imaging, Monash University, Building 220, Clayton Campus, 770 Blackburn Rd, Clayton, Victoria 3168, Australia. Email: anjan.bhattarai@monash.edu.

Background: Dysregulation of iron in the cerebral motor areas has been hypothesized to occur in individuals with amyotrophic lateral sclerosis (ALS). There is still limited knowledge regarding iron dysregulation in the progression of ALS pathology. Our objectives were to use magnetic resonance based quantitative susceptibility mapping (QSM) to investigate the association between iron dysregulation in the motor cortex and clinical manifestations in patients with limb-onset ALS, and to examine changes in the iron concentration in the motor cortex in these patients over a 6-month period.

Methods: Iron concentration was investigated using magnetic resonance based QSM in the primary motor cortex and the pre-motor area in 13 limb-onset ALS patients (including five lumbar onset, six cervical onset and two flail arm patients), and 11 age- and sex-matched control subjects. Nine ALS patients underwent follow-up scans at 6 months.

Results: Significantly increased QSM values were observed in the left posterior primary motor area (P=0.02, Cohen's d =0.9) and right anterior primary motor area (P=0.02, Cohen's d =0.92) in the group of limb-onset ALS patients compared to that of control subjects. Increased QSM was observed in the primary motor and pre-motor area at baseline in patients with lumbar onset ALS patients, but not cervical limb-onset ALS patients, compared to control subjects. No significant change in QSM was observed at the 6-month follow-up scans in the ALS patients.

Conclusions: The findings suggest that iron dysregulation can be detected in the motor cortex in limb-onset ALS, which does not appreciably change over a further 6 months. Individuals with lumbar onset ALS appear to be more susceptible to motor cortex iron dysregulation compared to the individuals with cervical onset ALS. Importantly, this study highlights the potential use of QSM as a quantitative radiological indicator in early disease diagnosis in limb-onset ALS and its subtypes. Our serial scans results suggest a longer period than 6 months is needed to detect significant quantitative changes in the motor cortex.

Keywords: Amyotrophic lateral sclerosis (ALS); iron; motor cortex; magnetic resonance imaging (MRI); quantitative susceptibility mapping (QSM)

Submitted Feb 10, 2020. Accepted for publication May 25, 2020.
doi: 10.21037/qims-20-187
View this article at: http://dx.doi.org/10.21037/qims-20-187

Introduction

Amyotrophic lateral sclerosis (ALS) is a relentlessly progressive, fatal neurodegenerative disease which is known to affect upper (UMN) and lower (LMN) motor neurons (1). Corticospinal tract (CST) degeneration and grey matter neuronal degeneration of the spinal cord, brain stem and motor cortex are considered to be the classical neuropathological features of ALS (2). The aetiology is largely unknown. A range of studies indicate that ALS neurodegeneration results from a complex interplay of excitotoxicity, oxidative stress, neuroinflammation, dysfunction of critical proteins and multiple genetic factors (2-4).

A number of studies have suggested iron homeostasis is impaired in the ALS brain (5,6). An *ex vivo* study reported increased iron accumulation, a prominent hallmark of neuroinflammation (7) in the microglia of the motor cortex in ALS patients (8). Increased levels of motor cortex iron accumulation have been associated with oxidative damage via the Fenton reaction (9,10). The Fenton reaction results in the formation of reactive oxygen species (hydroxyl radical) from a weak oxidant (hydrogen peroxide) in the presence of iron (ferrous ion) (9). The eventual result is neuronal cell degeneration (11), recently described as ferroptosis (an iron mediated cell death) (12). Further support for a deleterious effect of elevated iron in ALS has been found with a therapeutic effect of iron chelation in the superoxide dismutase-1 (SOD-1) mouse model of ALS (13). Given the evidence which suggests iron may play a significant role in the pathological process of ALS, an *in vivo* assessment of iron in disease progression in individuals with ALS may provide a pharmacodynamic marker for clinical trials.

Magnetic resonance imaging (MRI) has the capability to generate image contrast based on tissue magnetization that can map the neuroanatomical distribution of iron in the human brain. The development of quantitative susceptibility mapping (QSM) has enabled investigations of brain iron deposition *in vivo* (14,15). QSM is a relatively new magnetic resonance (MR) neuroimaging technique that allows the quantification of magnetic susceptibility using the phase of the MR signal (16). The magnetic susceptibility of tissue perturbs the apparent strength of an externally applied magnetic field and produces a detectable change in the phase of the MRI signal. Acquisition and post-processing MRI techniques have been developed to mathematically transform the non-local phase signal changes into voxel-based estimates of magnetic susceptibility in the brain. The QSM values are linearly proportional to the concentration of paramagnetic and diamagnetic species in a voxel (17), measured in parts per million (ppm) or parts per billion (ppb). The deposition of paramagnetic (or diamagnetic) species results in increased (or decreased) signal intensity in the QSM image. Iron within brain tissue is predominantly found in the paramagnetic form, and through QSM imaging has been quantified in a number of neurodegenerative diseases (17).

To date there have been seven published cross-sectional studies which have investigated iron in ALS using QSM alone and in combination with other MRI modalities (18-24). However, no longitudinal study has been undertaken to investigate changes in QSM values in ALS patients. Longitudinal QSM studies are needed to examine the role of iron in disease progression in ALS and to investigate potential differences in disease progression across the clinical ALS phenotypes.

This study aimed to determine the changes in iron concentration in the motor cortex of limb-onset ALS patients and its two clinical phenotypes; namely lumbar onset ALS and cervical onset ALS. In addition, we aimed to determine whether changes in iron concentration over 6 months in the motor cortex were associated with clinical progression in ALS. We anticipated that iron concentration in the motor cortex in limb-onset ALS would be increased compared to control subjects similar to results reported by other groups (8,21). Secondly, it was also expected that iron accumulation in the motor cortex in ALS patients would increase as the symptoms progressed as noted by previous studies (8,21). Furthermore, we hypothesized that there would be measurable changes in the concentration of iron in the motor cortex in ALS patients after 6 months of disease progression.

Methods

Ethics approval for this study was obtained from Calvary Health Care Bethlehem and Monash University Research Ethics Committees (Project Number: CF14/3968-2014002057).

Participants

We recruited participants over 18 years of age, who were able to give informed consent. Thirteen (2 females, 11 males) participants with clinically possible, probable

Table 1 Participant demographics and clinical scores (mean ± standard deviation)

Variables	ALS	Controls
Gender (F:M)	2:11	2:09
Age at baseline (years)	56.2±12.6	52.3±11.6
Age at follow-up (years)	59.5±11.0	NA
Number of participants at baseline	13	11
Number of participants at follow-up	13 (data available from 9)	NA
Baseline (cervical:lumbar:flail arm)	6:05:02	NA
Follow-up (cervical:lumbar:flail arm)	4:03:02	NA
Disease duration at baseline (years)[1]	3.8±3.8	NA
Disease duration at follow-up (years)	4.4±4.5	NA
ALSFRS-R1 (scores available from 11 participants which includes 6 cervical onset ALS, 4 lumbar onset ALS and 1 flail arm ALS)[2]	37.8±6.2	NA
ALSFRS-R2 (scores available from 8 participants which includes 4 cervical onset ALS, 3 lumbar onset ALS and 1 flail arm ALS)	34.8±9.4	NA

[1], disease duration based on patient report of symptom onset to time of baseline scan and follow-up scan; [2], ALSFRS-R1, and ALSFRS-R2 are ALSFRS-R scores at baseline and 6 months follow-up respectively. ALSFRS-R, ALS Functional Rating Scale Revised; ALS, amyotrophic lateral sclerosis; NA, not available.

or definite limb-onset ALS (cervical onset, n=6, lumbar onset n=5, flail arm phenotype n=2) and eleven (2 females, 9 males) age and gender matched control subjects underwent MRI scans. Control subjects were screened for neurological or psychiatric diseases. Nine patients with ALS participated in follow-up MR scans that were acquired 6 months after the initial scans. MR scans were not able to be successfully acquired for the other four ALS participants for the following reasons: one participant could not lie flat inside the MRI scanner for the follow-up scan, and data for the other three participants were irreversibly corrupted by a hardware storage failure. The participants with ALS underwent neurological assessments with the following clinical measures collected: the laterality and limb of onset, disease duration, and ALS Functional Rating Scale Revised (ALSFRS-R) as a measure of disease severity and progression (*Table 1*). The ALFRS-R data were collected at clinical visits and from the Australian Motor Neurone Disease Registry (AMNDR) database. Unfortunately, these data were not available for two patients (one lumbar onset ALS and one flail arm ALS) among 13 patients at baseline and one flail arm patient among nine patients at follow-up. All MRI scans of the ALS patients and control subjects were reviewed by a clinical radiologist. No clinically significant large lesions were noted in any of the scans included in the study.

MRI data acquisition

MRI data for the baseline and follow-up scans were acquired using a 3-Tesla Skyra MRI (Siemens, Erlangen, Germany) equipped with a 32-channel head-and-neck coil. The protocol included a T1-weighted magnetization prepared rapid gradient echo (MPRAGE) and a T2*-weighted gradient-recalled echo (GRE). The MPRAGE acquisition was performed using the following parameters: acquisition time =5 min 12 s, repetition time =2,300 ms, echo time =2.07 ms, flip angle =9°, field-of-view =256 mm, voxel size =1×1×1 mm^3, 192 slices per volume. The GRE sequence was performed with the following parameters: acquisition time =5 min 16 s, repetition time =30 ms, echo time =20 ms, flip angle =15°, field-of-view =230 mm, voxel size =0.9×0.9×1.8 mm^3, 72 slices per volume.

QSM processing

The phase and QSM processing was carried out using STI-Suite v2.2 (https://people.eecs.berkeley.edu/~chunlei.liu/software.html). Phase and magnitude images from each channel (coil) were reconstructed offline from raw

GRE *k*-space data. T2*-weighted magnitude images were calculated using a sum-of-squares coil combination for registration purposes. Bias correction was performed using N4 from Advanced Normalisation Tools (ANTs) (25). Brain masks were obtained using FSL-BET (26). The phase images from each coil were processed to remove phase warps using Laplacian Unwarping (voxel padding 12×12×12) (27,28). Background field was removed using V-SHARP (29,30). The processed phase images were combined using a magnitude-weighted average to produce a single-phase image as used previously (31). This approach will favor phase results from coils closest to each voxel whilst including information from all sources. QSM calculation was then performed using the improved sparse linear equation and least-squares algorithm (iLSQR) (32). In order to remove air tissue boundary artefacts in QSM, the brain mask was eroded using a spherical kernel with 5mm radius and multiplied with QSM image. QSM values were referenced to the whole brain mean magnetic susceptibility (33), and quantified as the mean in each region of interest (ROI). In order to exclude the susceptibility contributions from non-grey matter tissues, the mean QSM in each ROI was calculated including the voxels with magnetic susceptibility greater than 10 ppb (22).

ROIs

Subject-specific Brodmann area (BA) labels were obtained from the cortical parcellation of anatomical T1-weighted image using FreeSurfer (v6.0.0) (34,35). Two ROIs were used in the analysis: BA 4 (primary motor) and BA 6 (pre-motor). FreeSurfer cortical parcellation was performed on MASSIVE (36) using the "recon-all" function. The ROIs were: left and right anterior primary motor cortex (BA 4a), left and right posterior primary motor cortex (BA 4p) and pre-motor motor area (BA 6). The individual ROIs were checked and verified by an experienced neurologist (TG Phan) (*Figure 1*).

Image registration

For the registration of the ROIs to the QSM space, each participant's T1-weighted image was linearly co-registered to their T2*-weighted magnitude image using ANTs (37). The transformation matrices obtained from the linear registration were then applied to the motor cortex ROIs, originally in their respective MPRAGE space, to bring them to the participant's QSM space. For visual inspection and comparison, QSM images were registered to standard Montreal Neurological Institute (MNI) space using ANTs (37). The registered images are shown in *Figure 2*.

Statistical analyses

The ALS patients at baseline were further categorised into two subgroups on the basis of their individual clinical onset as either lumbar onset ALS or cervical onset ALS. Flail arm ALS was not included in the subgroup statistical analyses as our dataset contained only two such patients. Due to the small number of ALS patients with a follow-up scan, the patients with 6-month follow-up scans were not categorised on the basis of clinical onset or phenotype, and were analysed as a single group. Age related effects in the QSM measures were estimated in the control participant cohort and used to correct for normal age-related changes in the ALS patient cohorts. Group differences in QSM values between the ALS clinical phenotype cohorts and the control subjects were examined in the primary motor and pre-motor area ROIs. To test whether QSM was increased in limb-onset ALS (including lumbar onset, cervical onset, flail arm ALS) compared to control subjects, a non-parametric Wilcoxon rank sum test was used with the reported P values calculated in MATLAB using the "ranksum" function. The P value significance level was $P<0.05$ using a one-tailed distribution, and the comparisons between the ALS subgroups (lumbar and cervical onset ALS) with control subjects were corrected for multiple comparisons. The one-tailed distribution was chosen based an *ex vivo* study (8) and other QSM studies (20,21) which have found iron concentration to be elevated in the primary motor cortex of ALS patients compared to control subjects. To test whether QSM was changed at 6-month follow-up compared to baseline, a non-parametric Wilcoxon signed rank test was used with the reported P values (two-tailed) calculated in MATLAB using the "signrank" function. The P value significance level was $P<0.05$. The sample is paired such that QSM observations at baseline were considered only from the individuals whose follow-up observations were available.

Adjusted P values were calculated in MATLAB controlling the false discovery rate (FDR) following the Benjamini & Hochberg [1995] procedure (38). Unadjusted P values were reported in the following two instances. First, when comparing the baseline QSM values in limb-onset ALS (including lumbar onset, cervical onset, flail arm

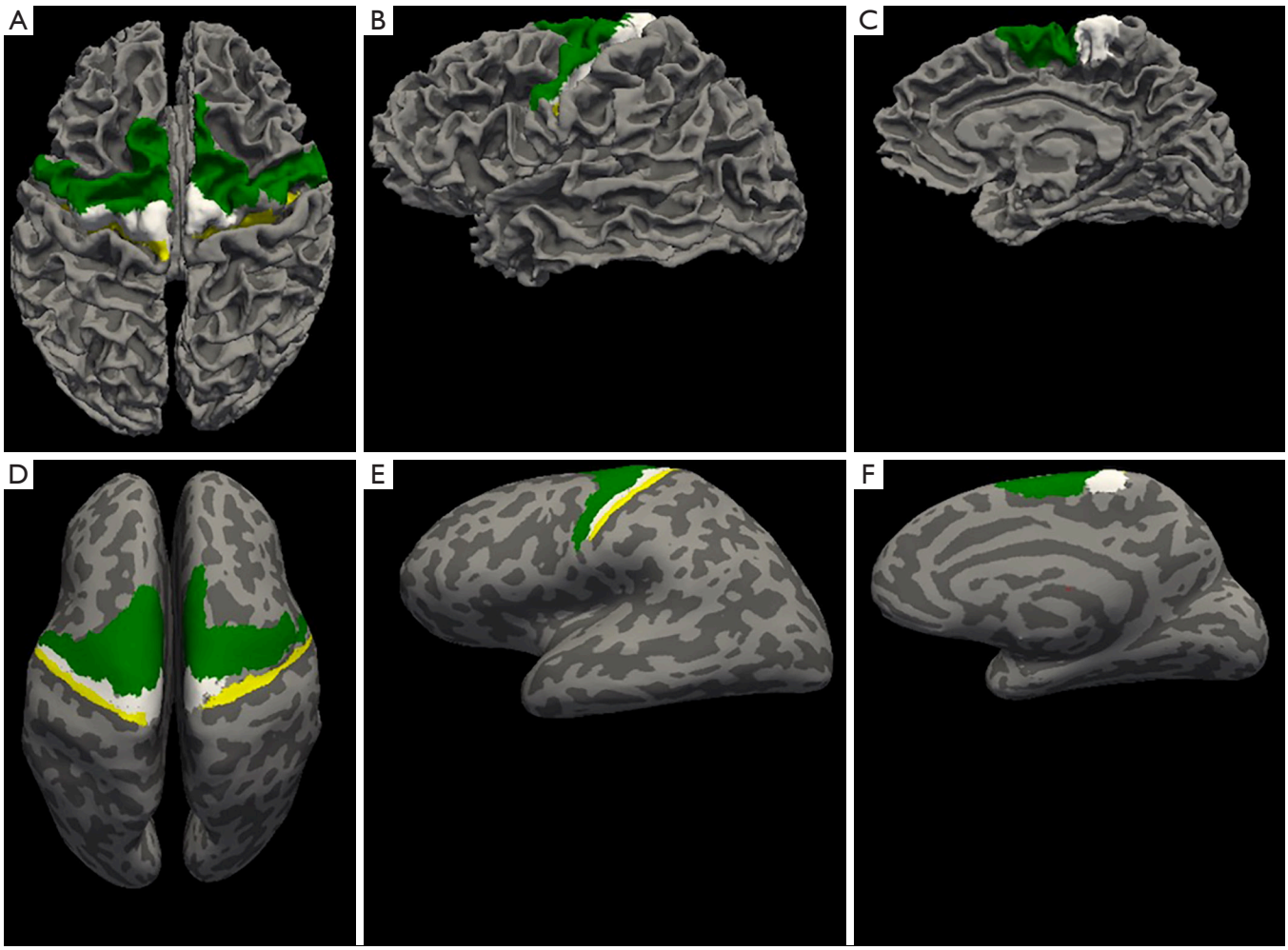

Figure 1 T1-weighted image based automated parcellation of the primary motor area (BA 4) and pre-motor area (Brodmann area 6) using FreeSurfer. The labels are anterior BA 4 (white), posterior BA 4 (yellow), pre-motor area (green). (A,B,C) shows top view, lateral view, and midsagittal view respectively of normal surface. (D,E,F) show top view, lateral view, and midsagittal view respectively of the inflated surface.

ALS) with control subjects. Second, when comparing the baseline QSM values and at 6-month follow-up due to the exploratory nature of the analysis with the small number of ALS patients. The QSM values are reported as group mean ± standard error of mean (SEM). The effect size was calculated using Cohen's d (39). The assumption of paired sample was considered to calculate the effect sizes while comparing baseline and follow-up QSM observations.

Correlations with disease duration and disease severity were assessed using non-parametric Spearman's rho (two-tailed). Disease duration was defined as the time between the date of disease onset based on patient report of symptom onset and the date of the MRI scan. Disease severity was quantified using ALSFRS-R scale (40). ALSFRS-R scores range from 0 to 48, where a score of 0 represents severely impaired and a score of 48 is unimpaired. All other parameters used in statistical analyses were set to default unless specified in the text. This study is underpowered to draw an inference from the correlation analyses with clinical measures but statistics are reported in the Supplementary material to facilitate future meta-analyses of this rare condition and its clinical subtypes.

Results

Significantly increased QSM values were observed in the group of individuals with limb-onset ALS compared to control subjects in the left posterior primary motor cortex

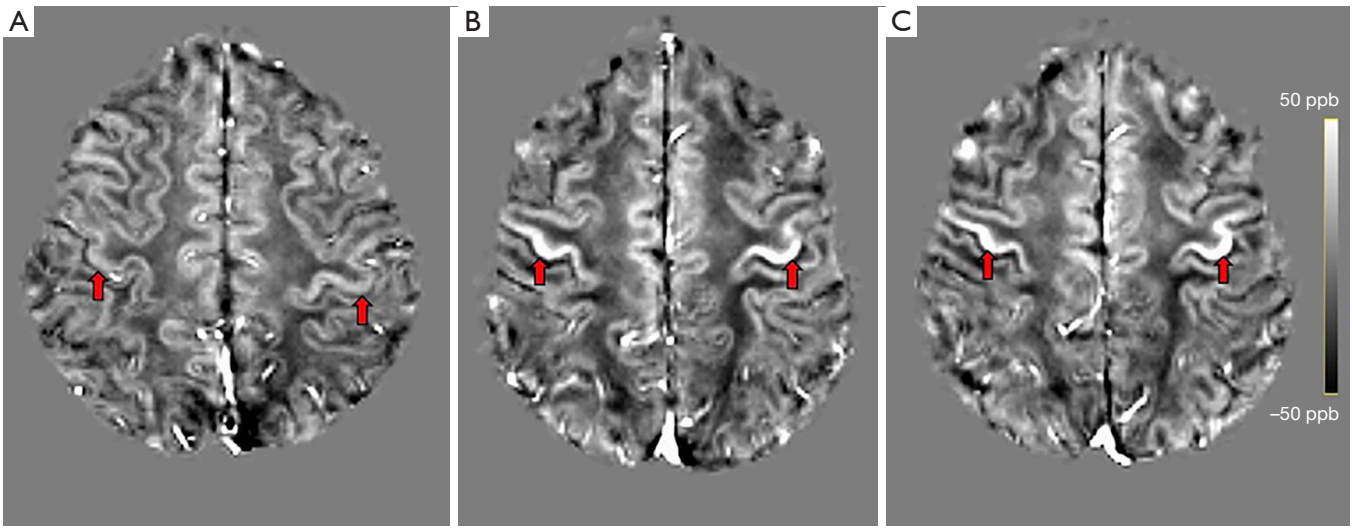

Figure 2 Hyperintense signal in the primary motor cortex (red arrows) in group-average QSM images for (A) a control subject, (B) an ALS patient at study entry, and (C) the same ALS patient at the 6 months follow-up scan. QSM, quantitative susceptibility mapping; ALS, amyotrophic lateral sclerosis.

and right anterior primary motor cortex (*Table 2*). Increased QSM values were observed in all other motor cortex regions of limb-onset ALS participants compared to control subjects but did not reach the level of statistical significance.

We observed an increased pattern of QSM values in the anterior primary motor area (bilateral), left posterior primary motor area and the right pre-motor area at baseline in patients with lumbar onset ALS compared to control subjects (*Table 3*) together with strong effect sizes (Cohen's d). The group differences in QSM values between the cervical onset ALS patients at baseline and the control subjects were not statistically significant (*Table 3*). The change in QSM values in limb-onset ALS participants between baseline and 6-month follow-up scans was not significant (*Table 4*).

Positive correlations were observed between disease duration and QSM values in all ROIs in limb-onset ALS at both baseline and follow-up but were not statistically significant (statistics are reported in the Supplementary material). Correlations between disease duration at baseline and QSM observations in lumbar and cervical onset ALS at baseline were not statistically significant. Progression in clinical symptoms did not reflect the change in QSM observations as we did not observe statistically significant anti-correlation between disease severity scores as measured by ALSFRS-R scale and QSM observations in limb-onset ALS and its subtypes. The statistics for correlation analyses are reported in the Supplementary material.

Discussion

In this study, we investigated motor cortex iron dysregulation in one of the common clinical phenotypes of ALS—limb-onset ALS using MR-based QSM and its two clinical subtypes: lumbar onset ALS and cervical onset ALS. We sought to minimize the heterogeneity by limiting our sample to a common clinical ALS phenotype. Our findings confirm the results of previous studies, where significantly increased iron levels were detected in the motor cortex in limb-onset ALS relative to control subjects (8,21). We observed that individuals with lumbar onset ALS had more motor cortex iron dysregulation than cervical onset ALS relative to control subjects. Although a larger cohort is needed to statistically test such differences, our preliminary results highlight the potential of using QSM to differentiate ALS subtypes. We explored the use of QSM as a radiological marker of disease progression. In our preliminary findings, we observed no detectable change in the iron concentration over 6 months of disease, and no significant correlation with disease duration. Our findings suggest that a potential minimal observation period greater than 6 months may be needed to observe significant changes in QSM. However, it is worthwhile to note that a larger cohort may be required to confirm these findings. Furthermore, even though we

Table 2 Summary of the cross-sectional age-corrected QSM observations. Statistical significance measured with Wilcoxon rank sum test (one-tailed)

ROI	QSM (ppb)		Baseline ALS *vs.* control subjects	
	Control subjects, mean ± SEM	Baseline ALS, mean ± SEM	P value	Cohen's d
Left primary motor area (anterior)	27.8±0.9	29.6±1.0	0.12	0.57
Right primary motor area (anterior)	29.7±1.1	33.0±0.9	0.02*	0.92
Left primary motor area (posterior)	27.0±0.8	30.2±1.2	0.02*	0.9
Right primary motor area (posterior)	28.3±0.8	30.3±1.1	0.09	0.58
Left pre-motor area	23.1±0.6	24.4±0.8	0.23	0.50
Right pre-motor area	23.2±0.5	24.6±1.0	0.09	0.47

QSM, quantitative susceptibility mapping; ALS, amyotrophic lateral sclerosis; SEM, standard error of the mean; ROI, region of interest.

have restricted our sample to limb-onset ALS, our group was still heterogeneous with respect to their ALSFRS scores. Whilst all motor cortical subregions in the baseline ALS patients presented increased QSM values compared to the control group, only the changes in right anterior and left posterior primary motor cortex were found to be statistically significant. This is likely due to the relatively small cohort size in this preliminary study, and studies with larger sample size are needed to confirm these findings.

Although limited with small sample size, this is the first study to investigate serial assessment of motor cortex iron dysregulation in limb-onset ALS. Given the heterogeneous presentation of ALS, our cohort was restricted to limb-onset ALS to enable a more focused exploration of the most common ALS clinical phenotype. Limb-onset ALS also has a longer duration of illness (41,42) such that all but one patient were able to be rescanned at 6 months.

Iron plays a significant role as a cofactor in many regulatory enzymes involved in the cellular metabolism process occurring in the mitochondria (8). Due to the high metabolic activity of the brain, iron has a prominent role in the central nervous system. Iron levels in the brain have been reported to increase as part of the normal ageing process (43). However, increased iron levels have also been observed in people diagnosed with neurodegenerative disorders such as Parkinson's disease (43), Friedreich Ataxia (44) and Alzheimer's disease (45). A pathological study conducted in two ALS patients (42 and 51 years) reported increased iron accumulation in the motor cortex despite their young age (8). Imaging findings of the same study showed hypointense signal in the deep layers of motor cortex in 7 Tesla MRI T2*-weighted gradient echo images in both patients, suggesting that the MRI signal alterations were due to the increased iron accumulation. Our study corroborates the findings of a cross-sectional study by Lee *et al.* [2017] which reported significantly higher QSM in the motor cortex of ALS patients compared to control subjects (20). Another cross-sectional study by Costagli *et al.* [2016] reported significantly higher magnetic susceptibility in M1 subregions of ALS patients compared to control subjects (21). They demonstrated a strong positive correlation between magnetic susceptibility and the expected concentration of iron in different cortical regions in control subjects. The expected concentration of iron in control subjects was calculated based on the findings of an earlier histological study (46). Their results were consistent with previous *ex vivo* findings which reported increased iron accumulation in microglial cells in the deep layers of the motor cortex (8). Qualitatively, the diagnostic accuracy of QSM in ALS compared to earlier MRI techniques such as T2-weighted, T2*-weighted and T2 FLAIR images has been demonstrated by Schweitzer *et al.* [2015], showing significantly greater motor cortex susceptibility in motor neurone disease (MND) patients [including both ALS and primary lateral sclerosis (PLS)] which was postulated to reflect increased iron accumulation (22). PLS is a less common progressive neurodegenerative disease which is known to affect UMN (47). Our study results are consistent

Table 3 Summary of the cross-sectional age-corrected QSM observations between control subjects and lumbar and cervical onset ALS respectively at baseline. Statistical significance measured with Wilcoxon rank sum test (one-tailed)

ROI	QSM (ppb)			Lumbar onset ALS *vs.* control subjects		Cervical onset ALS *vs.* control subjects	
	Control subjects, mean ± SEM	Lumbar onset ALS, mean ± SEM	Cervical onset ALS, mean ± SEM	P value adjusted	Cohen's d	P value adjusted	Cohen's d
Left primary motor area (anterior)	27.8±0.9	30.8±1.1	29.2±1.8	0.07	1.09	0.40	0.40
Right primary motor area (anterior)	29.7±1.1	34.4±1.9	32.5±1.2	0.07	1.21	0.36	0.81
Left primary motor area (posterior)	27.0±0.8	30.5±1.32	29.8±2.5	0.07	1.34	0.40	0.70
Right primary motor area (posterior)	28.3±0.8	31.2±1.5	30.2±2.0	0.07	1.01	0.40	0.52
Left pre-motor area	23.1±0.6	25.9±2.0	23.5±0.6	0.13	0.94	0.40	0.22
Right pre-motor area	23.2±0.53	26.6±2.2	23.1±0.6	0.07	1.12	0.40	−0.08

QSM, quantitative susceptibility mapping; ALS, amyotrophic lateral sclerosis; SEM, standard error of the mean; ROI, region of interest.

with these studies which indicate iron dysfunction in the motor cortex in ALS. Furthermore, the difference noted in lumbar onset ALS highlights the importance of studying subgroups of ALS as the distribution of iron mediated pathological mechanisms may be different.

There are methodological considerations to the current study. QSM is a nascent method undergoing rapid development (48) and importantly QSM provides relative rather than absolute values of magnetic susceptibility measurements. The *k*-space origin of the calculated susceptibility map during the QSM reconstruction process is mathematically unconstrained. As a result, the QSM susceptibility map has an unknown offset so the susceptibility values must be referenced to a particular brain region or tissue (49). In this study, the QSM values reported were referenced to whole brain mean susceptibility value rather than the susceptibility of specific anatomical region, in order to minimize any potential biases that may result from disease related susceptibility changes in a specific reference region. However, it is unknown whether the whole brain mean appreciably changes longitudinally in ALS and any such change may obscure the findings of this study. The QSM values amongst studies also differ depending upon the methods and parameters used for phase processing, as well as the magnetic field strength, imaging protocols and equipment used for MRI data acquisition (50-55). Furthermore, QSM measurements can potentially depend on tissue structural orientation (56). These factors can impact on the QSM values between different published studies but do not have any impact on the significance of group difference and longitudinal changes within a single study. Further developments towards protocol and processing standardization may mitigate these factors and improve the reliability of QSM analyses from multi-center studies.

The current study has several limitations. The study was conducted in relatively small sized cohorts of patients with clinically possible, probable or definite limb-onset ALS. Follow-up MRI data were available for only nine out of thirteen patients. Whilst larger sample sizes would contribute to higher statistical power for between group analyses, the rarity and rapid progression of the disease make large cohort studies difficult. For the longitudinal analysis, MRI data were available for two time points with a relatively short duration of 6-month between the scans. Although we chose to study only limb-onset ALS, the cohort was still heterogeneous with respect to disease stages, disease duration and clinical symptoms of ALS. Future longitudinal studies over a longer time span are

Table 4 Summary of the serial age-corrected QSM observations. Statistical significance measured with Wilcoxon signed rank test (two-tailed). The assumption of paired sample was considered while calculating the effect sizes

ROI	QSM (ppb)		Baseline ALS *vs.* 6 months	
	Baseline ALS, mean ± SEM	6 months ALS, mean ± SEM	P value	Cohen's d
Left primary motor area (anterior)	30±1.3	29.9±1.3	1	–0.03
Right primary motor area (anterior)	33.7±1.2	34.4±1.9	0.73	0.23
Left primary motor area (posterior)	31.2±1.6	29.9±1.4	0.05	–0.77
Right primary motor area (posterior)	31±1.5	31.3±2	0.91	0.13
Left pre-motor area	24.6±1.2	25.2±1.3	0.3	0.56
Right pre-motor area	25.1±1.4	25.7±1.4	0.05	0.76

QSM, quantitative susceptibility mapping; ALS, amyotrophic lateral sclerosis; SEM, standard error of the mean; ROI, region of interest.

needed to examine the trajectory of iron accumulation in ALS, although unfortunately such studies will be limited by the short prognosis in most patients with ALS and the concomitant difficulty of lying flat in the MRI scanner as the disease progresses.

Conclusions

This study demonstrates the efficacy of QSM to detect iron concentration differences in the motor cortex of individuals with limb-onset ALS. The results suggest that iron levels are significantly increased in the primary motor cortex in limb-onset ALS relative to control subjects, and the changes may not show significant progression over a 6-month period. Increased iron concentration was observed in the pre-motor areas in ALS patients, but the difference with respect to control subjects was not statistically significant. Analysis of iron concentration can provide meaningful insights into the pathological process of ALS. Future longitudinal studies with multiple scans, performed over longer periods in a larger cohort, grouped on the basis of disease stage, severity, clinical presentations and phenotypes are required to further explore the role of iron in the degeneration process.

Acknowledgments

We would like to thank all the volunteers who participated in this study. We are also grateful to the radiographers at Monash Biomedical Imaging for their assistance with MRI data collection and our nurse research assistants Ruth Krasniqi and Anna Smith. Funding: Funding for this project was obtained through the Monash University Strategic Grant Scheme. AB was supported by The Australian Rotary Health/Rotary Club of Sandy Bay PhD Scholarship in Motor Neuron Disease.

Footnote

Conflicts of Interest: All authors have completed the ICMJE uniform disclosure form (available at http://dx.doi.org/10.21037/qims-20-187). The authors have no conflicts of interest to declare.

Ethical Statement: Ethics approval for this study was obtained from Calvary Health Care Bethlehem and Monash University Research Ethics Committees (Project Number: CF14/3968-2014002057). Written informed consent was obtained from the patients for publication of this study and any accompanying images. A copy of the written consent is available for review by the Editor-in-Chief of this journal.

References

1. Kiernan MC, Vucic S, Cheah BC, Turner MR, Eisen A, Hardiman O, Burrell JR, Zoing MC. Amyotrophic lateral sclerosis. Lancet 2011;377:942-55.
2. Wang S, Melhem ER, Poptani H, Woo JH. Neuroimaging in amyotrophic lateral sclerosis. Neurotherapeutics 2011;8:63-71.
3. Bonafede R, Mariotti R. ALS Pathogenesis and Therapeutic Approaches: The Role of Mesenchymal Stem Cells and Extracellular Vesicles. Front Cell Neurosci 2017;11:80.
4. Carrí MT, Ferri A, Cozzolino M, Calabrese L, Rotilio G. Neurodegeneration in amyotrophic lateral sclerosis: the role of oxidative stress and altered homeostasis of metals. Brain Res Bull 2003;61:365-74.
5. Hadzhieva M, Kirches E, Wilisch-Neumann A, Pachow D, Wallesch M, Schoenfeld P, Paege I, Vielhaber S, Petri S, Keilhoff G, Mawrin C. Dysregulation of iron protein expression in the G93A model of amyotrophic lateral sclerosis. Neuroscience 2013;230:94-101.
6. Oshiro S, Morioka MS, Kikuchi M. Dysregulation of iron metabolism in Alzheimer's disease, Parkinson's disease, and amyotrophic lateral sclerosis. Adv Pharmacol Sci 2011;2011:378278.
7. Nnah IC, Wessling-Resnick M. Brain Iron Homeostasis: A Focus on Microglial Iron. Pharmaceuticals 2018;11:129.
8. Kwan JY, Jeong SY, Van Gelderen P, Deng HX, Quezado MM, Danielian LE, Butman JA, Chen L, Bayat E, Russell J, Siddique T, Duyn JH, Rouault TA, Floeter MK. Iron accumulation in deep cortical layers accounts for MRI signal abnormalities in ALS: correlating 7 tesla MRI and pathology. PLoS One 2012;7:e35241.
9. Contestabile A. Amyotrophic lateral sclerosis: from research to therapeutic attempts and therapeutic perspectives. Curr Med Chem 2011;18:5655-65.
10. Jomova K, Vondrakova D, Lawson M, Valko M. Metals, oxidative stress and neurodegenerative disorders. Mol Cell Biochem 2010;345:91-104.
11. Petri S, Korner S, Kiaei M. Nrf2/ARE Signaling Pathway: Key Mediator in Oxidative Stress and Potential Therapeutic Target in ALS. Neurol Res Int 2012;2012:878030.
12. Masaldan S, Bush AI, Devos D, Rolland AS, Moreau C. Striking while the iron is hot: Iron metabolism and ferroptosis in neurodegeneration. Free Radic Biol Med 2019;133:221-33.
13. Wang Q, Zhang X, Chen S, Zhang X, Zhang S, Youdium M, Le W. Prevention of motor neuron degeneration by novel iron chelators in SOD1(G93A) transgenic mice of amyotrophic lateral sclerosis. Neurodegener Dis 2011;8:310-21.
14. Salomir R, de Senneville BD, Moonen CT. A fast calculation method for magnetic field inhomogeneity due to an arbitrary distribution of bulk susceptibility. Concepts Magn Reson 2003;19B:26-34.
15. Marques J, Bowtell R. Application of a Fourier-based method for rapid calculation of field inhomogeneity due to spatial variation of magnetic susceptibility. Concepts Magn Reson 2005;25B:65-78.
16. Haacke EM, Liu S, Buch S, Zheng W, Wu D, Ye Y. Quantitative susceptibility mapping: current status and future directions. Magn Reson Imaging 2015;33:1-25.
17. Duyn JH, Schenck J. Contributions to magnetic susceptibility of brain tissue. NMR Biomed 2017;30. doi:10.1002/nbm.3546.
18. Weidman EK, Schweitzer AD, Niogi SN, Brady EJ, Starikov A, Askin G, Shahbazi M, Wang Y, Lange D, Tsiouris AJ. Diffusion tensor imaging and quantitative susceptibility mapping as diagnostic tools for motor neuron disorders. Clin Imaging 2019;53:6-11.
19. Acosta-Cabronero J, Machts J, Schreiber S, Abdulla S, Kollewe K, Petri S, Spotorno N, Kaufmann J, Heinze HJ, Dengler R, Vielhaber S, Nestor PJ. Quantitative Susceptibility MRI to Detect Brain Iron in Amyotrophic Lateral Sclerosis. Radiology 2018;289:195-203.
20. Lee JY, Lee YJ, Park DW, Nam Y, Kim SH, Park J, Kim YS, Kim HY, Oh KW. Quantitative susceptibility mapping of the motor cortex: a comparison of susceptibility among patients with amyotrophic lateral sclerosis, cerebrovascular disease, and healthy controls. Neuroradiology 2017;59:1213-22.
21. Costagli M, Donatelli G, Biagi L, Caldarazzo Ienco E, Siciliano G, Tosetti M, Cosottini M. Magnetic susceptibility in the deep layers of the primary motor cortex in Amyotrophic Lateral Sclerosis. Neuroimage Clin 2016;12:965-9.
22. Schweitzer AD, Liu T, Gupta A, Zheng K, Seedial S, Shtilbans A, Shahbazi M, Lange D, Wang Y, Tsiouris AJ. Quantitative susceptibility mapping of the motor cortex in amyotrophic lateral sclerosis and primary lateral sclerosis. AJR Am J Roentgenol 2015;204:1086-92.
23. Welton T, Maller JJ, Lebel RM, Tan ET, Rowe DB, Grieve SM. Diffusion kurtosis and quantitative susceptibility mapping MRI are sensitive to structural abnormalities in amyotrophic lateral sclerosis. Neuroimage

Clin 2019;24:101953.
24. Donatelli G, Caldarazzo Ienco E, Costagli M, Migaleddu G, Cecchi P, Siciliano G, Cosottini M. MRI cortical feature of bulbar impairment in patients with amyotrophic lateral sclerosis. Neuroimage Clin 2019;24:101934.
25. Tustison NJ, Avants BB, Cook PA, Zheng Y, Egan A, Yushkevich PA, Gee JC. N4ITK: improved N3 bias correction. IEEE Trans Med Imaging 2010;29:1310-20.
26. Smith SM. Fast robust automated brain extraction. Hum Brain Mapp 2002;17:143-55.
27. Li W, Wu B, Liu C. Quantitative susceptibility mapping of human brain reflects spatial variation in tissue composition. Neuroimage 2011;55:1645-56.
28. Schofield MA, Zhu Y. Fast phase unwrapping algorithm for interferometric applications. Opt Lett 2003;28:1194-6.
29. Schweser F, Deistung A, Lehr BW, Reichenbach JR. Quantitative imaging of intrinsic magnetic tissue properties using MRI signal phase: an approach to in vivo brain iron metabolism? Neuroimage 2011;54:2789-807.
30. Wu B, Li W, Guidon A, Liu C. Whole brain susceptibility mapping using compressed sensing. Magn Reson Med 2012;67:137-47.
31. Ward PGD, Ferris NJ, Raniga P, Dowe DL, Ng ACL, Barnes DG, Egan GF. Combining images and anatomical knowledge to improve automated vein segmentation in MRI. Neuroimage 2018;165:294-305.
32. Li W, Wang N, Yu F, Han H, Cao W, Romero R, Tantiwongkosi B, Duong TQ, Liu C. A method for estimating and removing streaking artifacts in quantitative susceptibility mapping. Neuroimage 2015;108:111-22.
33. Straub S, Schneider TM, Emmerich J, Freitag MT, Ziener CH, Schlemmer HP, Ladd ME, Laun FB. Suitable reference tissues for quantitative susceptibility mapping of the brain. Magn Reson Med 2017;78:204-14.
34. Fischl B. FreeSurfer. Neuroimage 2012;62:774-81.
35. Fischl B, Rajendran N, Busa E, Augustinack J, Hinds O, Yeo BT, Mohlberg H, Amunts K, Zilles K. Cortical folding patterns and predicting cytoarchitecture. Cereb Cortex 2008;18:1973-80.
36. Goscinski WJ, McIntosh P, Felzmann U, Maksimenko A, Hall C, Gureyev T, Thompson D, Janke A, Galloway G, Killeen N, Raniga P, Kaluza O, Ng A, Poudel G, Barnes D, Nguyen T, Bonnington P, Egan G. The multi-modal Australian ScienceS Imaging and Visualization Environment (MASSIVE) high performance computing infrastructure: applications in neuroscience and neuroinformatics research. Front Neuroinform 2014;8:30.
37. Avants BB, Epstein CL, Grossman M, Gee JC. Symmetric diffeomorphic image registration with cross-correlation: evaluating automated labeling of elderly and neurodegenerative brain. Med Image Anal 2008;12:26-41.
38. Benjamini Y, Hochberg Y. Controlling The False Discovery Rate - A Practical And Powerful Approach To Multiple Testing. J R Stat Soc Series B Stat Methodol 1995;57:289-300.
39. Cohen J. Statistical Power Analysis for the Behavioral Sciences. 2nd edition. Abingdon, UK: Taylor & Francis, 2013.
40. Cedarbaum JM, Stambler N, Malta E, Fuller C, Hilt D, Thurmond B, Nakanishi A. The ALSFRS-R: a revised ALS functional rating scale that incorporates assessments of respiratory function. BDNF ALS Study Group (Phase III). J Neurol Sci 1999;169:13-21.
41. Turner MR, Parton MJ, Shaw CE, Leigh PN, Al-Chalabi A. Prolonged survival in motor neuron disease: a descriptive study of the King's database 1990-2002. J Neurol Neurosurg Psychiatry 2003;74:995-7.
42. Turner MR, Brockington A, Scaber J, Hollinger H, Marsden R, Shaw PJ, Talbot K. Pattern of spread and prognosis in lower limb-onset ALS. Amyotroph Lateral Scler 2010;11:369-73.
43. Zecca L, Youdim MB, Riederer P, Connor JR, Crichton RR. Iron, brain ageing and neurodegenerative disorders. Nat Rev Neurosci 2004;5:863-73.
44. Ward PGD, Harding IH, Close TG, Corben LA, Delatycki MB, Storey E, Georgiou-Karistianis N, Egan GF. Longitudinal evaluation of iron concentration and atrophy in the dentate nuclei in friedreich ataxia. Mov Disord 2019;34:335-43.
45. Rouault TA, Cooperman S. Brain iron metabolism. Semin Pediatr Neurol 2006;13:142-8.
46. Hallgren B, Sourander P. The effect of age on the non-haemin iron in the human brain. J Neurochem 1958;3:41-51.
47. Tartaglia MC, Rowe A, Findlater K, Orange JB, Grace G, Strong MJ. Differentiation between primary lateral sclerosis and amyotrophic lateral sclerosis: examination of symptoms and signs at disease onset and during follow-up. Arch Neurol 2007;64:232-6.
48. Langkammer C, Schweser F, Shmueli K, Kames C, Li X, Guo L, Milovic C, Kim J, Wei H, Bredies K, Buch S, Guo Y, Liu Z, Meineke J, Rauscher A, Marques JP, Bilgic B. Quantitative susceptibility mapping: Report from the 2016 reconstruction challenge. Magn Reson Med 2018;79:1661-73.
49. Deistung A, Schweser F, Reichenbach JR. Overview

of quantitative susceptibility mapping. NMR Biomed 2017;30:e3569.
50. Lancione M, Donatelli G, Cecchi P, Cosottini M, Tosetti M, Costagli M. Echo-time dependency of quantitative susceptibility mapping reproducibility at different magnetic field strengths. Neuroimage 2019;197:557-64.
51. Cronin MJ, Wang N, Decker KS, Wei H, Zhu WZ, Liu C. Exploring the origins of echo-time-dependent quantitative susceptibility mapping (QSM) measurements in healthy tissue and cerebral microbleeds. Neuroimage 2017;149:98-113.
52. Sood S, Urriola J, Reutens D, O'Brien K, Bollmann S, Barth M, Vegh V. Echo time-dependent quantitative susceptibility mapping contains information on tissue properties. Magn Reson Med 2017;77:1946-58.
53. Zhou D, Cho J, Zhang J, Spincemaille P, Wang Y. Susceptibility underestimation in a high-susceptibility phantom: Dependence on imaging resolution, magnitude contrast, and other parameters. Magn Reson Med 2017;78:1080-6.
54. Karsa A, Punwani S, Shmueli K. The effect of low resolution and coverage on the accuracy of susceptibility mapping. Magn Reson Med 2019;81:1833-48.
55. Elkady AM, Sun H, Wilman AH. Importance of extended spatial coverage for quantitative susceptibility mapping of iron-rich deep gray matter. Magn Reson Imaging 2016;34:574-8.
56. Lancione M, Tosetti M, Donatelli G, Cosottini M, Costagli M. The impact of white matter fiber orientation in single-acquisition quantitative susceptibility mapping. NMR Biomed 2017;30. doi: 10.1002/nbm.3798.

Cite this article as: Bhattarai A, Chen Z, Ward PGD, Talman P, Mathers S, Phan TG, Chapman C, Howe J, Lee S, Lie Y, Egan GF, Chua P. Serial assessment of iron in the motor cortex in limb-onset amyotrophic lateral sclerosis using quantitative susceptibility mapping. Quant Imaging Med Surg 2020;10(7):1465-1476. doi: 10.21037/qims-20-187

Supplementary

Estimation and correction for age-related changes in QSM

Age related effects in the QSM measures were estimated in the control participant cohort and used to correct for normal age-related changes in the ALS patient cohorts.

Age corrected QSM = Uncorrected QSM – b × (age – mean age), where b is the slope of a regression and mean age is the mean age of controls subjects.

b is calculated using linear regression in SPSS, choosing uncorrected QSM of control subjects for each ROI as dependent variable and age of the control subjects as independent variable. The unstandardized B is the value for b.

Statistics for clinical correlation (*Table S1*)

Table S1 Summary of the correlations between clinical measures (disease duration and disease severity, i.e., ALSFRS-R score) and age corrected QSM observations

ROI	Disease duration *vs.* QSM								ALSFRS-R *vs.* QSM							
	Correlation at baseline						Correlation at follow-up		Correlation at baseline						Correlation at follow-up	
	ALS		Lumbar onset ALS		Cervical onset ALS		ALS		ALS		Lumbar onset ALS		Cervical onset ALS		ALS	
	rho	P	rho	P	rho	P	rho	P	rho	P	rho	P	rho	P	rho	P
Left primary motor area (anterior)	0.09	0.76	0	1.00	0.54	0.30	0.40	0.29	0.43	0.18	0.8	0.33	–0.14	0.80	–0.05	0.92
Right primary motor area (anterior)	0.08	0.81	–0.1	0.95	0.31	0.56	0.23	0.55	0.37	0.26	0.8	0.33	0.09	0.92	–0.01	0.99
Left primary motor area (posterior)	0.27	0.37	0.7	0.23	–0.03	1.00	0.20	0.61	0.39	0.24	1.0	0.08	0.09	0.92	–0.13	0.76
Right primary motor area (posterior)	0.15	0.63	–0.1	0.95	0.14	0.80	0.23	0.55	0.38	0.25	0.6	0.42	0.31	0.56	0.08	0.85
Left pre-motor area	0.03	0.94	–0.1	0.95	0.26	0.66	0.13	0.74	0.32	0.34	0.8	0.33	–0.43	0.42	0.02	0.96
Right pre-motor area	0.15	0.62	–0.2	0.78	0.60	0.24	0.42	0.27	0.66	0.03*	0.6	0.42	0.49	0.36	0.55	0.16

ALSFRS-R, ALS Functional Rating Scale Revised; QSM, quantitative susceptibility mapping; ALS, amyotrophic lateral sclerosis; ROI, region of interest.